General and Comparative Endocrinology 277 (2019) 30–37

Contents lists available at ScienceDirect

General and Comparative Endocrinology

journal homepage: www.elsevier.com/locate/ygcen

Identification, characterization, expression profiles of *OlHavcr2* in medaka (*Oryzias latipes*)

Emile Nibona, Gongyu Xu, Kongyue Wu, Hao Shen, Runshuai Zhang, Xiaomei Ke, Abdullah Al Hafiz, Zequn Wang, Chao Qi, Haobin Zhao*

Hubei Key Laboratory of Genetic Regulation and Integrative Biology, School of Life Sciences, Central China Normal University, Wuhan 430079, Hubei, China

ARTICLE INFO

Keywords:
Havcr2
Medaka
Protein structure
Gene expression
Immune response

ABSTRACT

Hepatitis A virus cellular receptor2 (Havcr2) also named T-cell immunoglobulin and mucin domain containing-3 (Tim-3) was initially described as a T helper 1-specific cell surface protein, a member of Tim family implicated in the regulating process of adaptive and innate immune responses. Here, medaka (*Oryzias latipes*) *Havcr2* (*OlHavcr2*) was isolated and characterized. Unlike other Havcr2 proteins, OlHavcr2 possesses two Ig-like domains but lacks cytoplasmic and transmembrane domains. RT-PCR results revealed that *OlHavcr2* mRNA was expressed strongly in the liver, moderately in the intestine, heart and ovary, and weakly in the muscle, gill, brain, eye, spleen, and testis. *OlHavcr2* expression begun from gastrula stage and was maintained until hatching. The signal of *OlHavcr2* was mainly identified in the blood system in the yolk sac by in situ hybridization. These results indicated that *OlHavcr2* is expressed ubiquitously in adult tissues, and is a zygotic gene expressed from gastrula onwards in embryogenesis. OlHavcr2 may play a significant role in the blood system of medaka. In the immune organs, *OlHavcr2* expression was affected by the immune stimulants, lipopolysaccharide and poly I:C, suggesting that OlHavcr2 was involved in innate immunity and adaptive immunity in medaka.

1. Introduction

Hepatitis A virus cellular receptor 2 (*Havcr2*) is a gene that encodes a Havcr2 protein, also named T-cell immunoglobulin and mucin domain containing-3 (Tim-3). Originally, it was described as a T helper 1-specific cell surface protein (Monney et al., 2002; Sánchez-Fueyo et al., 2003), and later reported with the expression on T helper 17 cells (Nakae et al., 2007a,b) and innate immune cells including mast cells (Nakae et al., 2007a,b), macrophages (Anderson et al., 2007), and dendritic cells (DC) (Rodriguez-Manzanet et al., 2009) in mice. Human innate immune system expresses HAVCR2 on natural killer cells, monocytes (Chae et al., 2004), T-cells (Gao et al., 2012), and DC (Anderson et al., 2007). In murine, Havcr2 can stimulate macrophage in experimental autoimmune encephalomyelitis (Anderson et al., 2007). Moreover, Havcr2 is known as an immune checkpoint receptor involved in the immune homeostasis and can regulate innate and adaptive immunity (Hu et al., 2016; Yang et al., 2013).

HAVCR2 is involved in carcinogenesis and up-regulated in tumor-infiltrating lymphocytes in lung (Gao et al., 2012), gastric (Lu et al., 2017), ovarian (Yan et al., 2013), prostate (Japp et al., 2015), breast (Zhang et al., 2017), bone (Feng and Guo, 2016), neck and head cancer (Shayan et al., 2017), cytotoxic T cells of malignant schwannomas (Li et al., 2017), melanoma (Fourcade et al., 2010), and follicular B-cell non-Hodgkin lymphoma (Yang et al., 2012). Moreover, numerous studies proved the critical roles of HAVCR2 in suppressing rejection of transplanted skin (Sánchez-Fueyo et al., 2003), pancreatic islets (Sánchez-Fueyo et al., 2003), bone marrow allografts (Veenstra et al., 2012), and heart (Boenisch et al., 2010).

Havcr2 belongs to the *Tim* family that consists of *TIM-1* (*HAVCR1*), *TIM-3* (*HAVCR2*), and *TIM-4* located on chromosome 5 in human, and *Tim-1* to *Tim-8* (eight members) in the mouse chromosome 11 (McIntire et al., 2004). Previous findings have already shown that the members of the Tim family are engaged in the regulation of adaptive and innate immune responses, including asthma, autoimmunity, allergy, infection tolerance, and viral infections (Freeman et al., 2010; Hu et al., 2016; Li et al., 2013; Liu et al., 2017; Wang et al., 2017). The Tim or Kim (kidney injury molecule) members, Havcr1 (Tim-1/Kim1), Havcr2 (Tim-3/Kim3) and Tim-4 (Kim4) had been identified in zebrafish (Xu et al., 2016; Yin et al., 2016). Induction of Havcr1 in zebrafish kidney tubules resulted in kidney injury and increase of mortality (Yin et al., 2016). Havcr1 and Tim-4 also showed their conserved role in the development of T-cells in zebrafish (Xu et al., 2016). However, to the best of our

* Corresponding author.
E-mail address: zhaohb@mail.ccnu.edu.cn (H. Zhao).

https://doi.org/10.1016/j.ygcen.2018.10.023
Received 16 July 2018; Received in revised form 10 October 2018; Accepted 30 October 2018
Available online 03 November 2018
0016-6480/

knowledge, Havcr2 has not been well studied in fish to date.

In this study, medaka (*Oryzias latipes*), a common model fish was chosen as the subject. Medaka *Havcr2* (*OlHavcr2*) was isolated by reverse transcription polymerase chain reaction (RT-PCR). Bioinformatic analysis showed the unique character of OlHavcr2 with two Ig-like domains and without transmembrane domain and cytoplasm domain. Expressional analyses reveal that *OlHavcr2* is ubiquitously expressed in adult tissues and is a zygotic gene expressed from gastrula onwards during embryonic development.

2. Materials and methods

2.1. Experimental fish

Adult medaka were raised in circulating water baths at 28 °C under standard laboratory conditions. They were fed three times per day and maintained under an artificial photoperiod of 14 h of light and 10 h of darkness. The spontaneously spawned eggs were collected and incubated at 28.0 °C. The stages of embryos development were determined according to the criteria developed by Iwamatsu (Iwamatsu Takashi, 1994). Adult fish were arbitrarily sampled and sacrificed for RNA extraction.

2.2. Getting of OlHavcr2 gene from medaka

Previously, a fragment of a gene was identified as the bait of Prmt5 in the experiment of yeast two hybridization (Zhang et al., unpublished). By blasting the gene fragment in the database of National Center for Biotechnology Information (NCBI, https://www.ncbi.nlm.nih.gov/), a gene annotated as Coxsackie virus and adenovirus receptor (Cxadr)-like membrane protein (XM_004076668) was identified in medaka.

The open reading frame (ORF) of this gene was amplified by RT-PCR using specially designed primers namely *Havcr2*-F and *Havcr2*-R on XM_004076668 (Table 1). Total RNA from adult fish was isolated using TRIzol Reagent (Invitrogen) and was reversely transcribed to cDNA using FastQuant RT Kit (Tiangen Biotech (Beijing) Co., Ltd). To obtain the 3′- unknown region, the rapid amplification of cDNA end (RACE) technology was adopted by using SMARTer® RACE Kit (Takara). The gene-specific primers for 3′-RACE were designed on the ORF sequence obtained as above (Table 1). Purified RT-PCR product was sub-cloned into a pMD18-T vector (Takara) for sequencing. Full sequence was assembled with the RT-PCR and 3′-RACE results by software Lasergene Seqman. The ORF and the untranslated region (UTR) were searched by using Lasergene SeqBuilder software. The Primer Premier 5 software was employed to design the primers used in the present study.

Table 1
Primers used in this study.

Primer	Sequence (5′–3′)	Use
OlHavcr2-F	ATGAAGATCCTGGTGCTGCT	ORF Cloning and Gene expression
OlHavcr2-R	TCACTTTCTGTTGCGGGTTC	
β-actin-F	TCCGGTATGTGCAAAGCCGG	Gene expression
β-actin-R	CCACATCTGCTGGAAGGTGG	
*OlHavcr2*_q-F	AGGACAATACTTCTTAGGCTGC	qRT-PCR
*OlHavcr2*_q-R	TTCACTCTGCATGCGTACA	
S18-F	GTGTGGTGACCATCATGCAGAA	qRT-PCR
S18-R	TGGCAAGGACCTGGCTGTATT	
OlHavcr2-ISH-F	CACAGAGGAAGATGCTGGAAT	ISH-probe
OlHavcr2-ISH-R	CAGATGAGAAACAGAACCTT	
3′ GSP-F	GATTACGCCAAGCTTCCTCTGACTG CGACGATGACGGAAT	3′-RACE

2.3. Bioinformatics analyses

The homologs and identities were retrieved through the NCBI website. The gene sequence was mapped onto genomic DNA by Ensembl genome browser. The phylogenetic tree and the estimate divergences between various protein sequences were built and calculated using MEGA7 (Kumar et al., 2016). The signal peptide, N-linked glycosylation sites, and O-linked glycosylation positions were predicted by using SignalP 4.1 server (Nielsen et al., 1997), NetNGlyc 1.0 server (Blom et al., 2004) and NetOGlyc 4.0 server (Steentoft et al., 2013) respectively. The Ig-like domain, mucin domain, cytoplasmic domain, and transmembrane domain were determined by using the Simple Molecular Architecture Research Tools (SMART) (Letunic et al., 2015; Schultz et al., 1998). The tertiary structures were obtained by using SWISS-MODEL and PyMOL software.

2.4. RT-PCR for expression analysis of OlHavcr2

Total RNA was extracted from different tissues including the muscle, eye, spleen, brain, gill, testis, heart, intestine, liver and ovary, and the embryos at various stages of development. The cDNA was synthesized as described above. Routine RT-PCR reaction system was in a total volume of 25.0 μL containing 12.5 μL of 2 × Es Taq MasterMix, 1.0 μL of each primer (*Havcr2*-F and *Havcr2*-R, Table 1), 1.0 μL of cDNA and 9.5 μL of H_2O. Cycling program was 94 °C for 5 min, followed by 30 cycles of 94 °C for 30 s, 57 °C for 30 s, 72 °C for 70 s, with the last extension for 10 min at 72 °C. The product was then run on agarose gel and documented.

Quantities of *OlHavcr2* were also measured on the adult tissues and embryos using quantitative real-time PCR (qRT-PCR) with primers *OlHavcr2_q*-F and *OlHavcr2_q*-R (Table 1). A volume of 20.0 μL reaction system was established according to the SuperReal PreMix Plus (SYBR Green) Kit (Tiangen): 10.0 μL of 2× SuperReal PreMix Plus, 0.6 μL of each qRT-PCR primer, 4.0 μL diluted cDNA and 4.8 μL of H_2O. QRT-PCR conditions were 95 °C for 3 min, followed by 42 cycles at 95 °C for 10 s, 56 °C for 20 s and 72 °C for 30 s. The relative expression of the gene was determined by using the $2^{-\Delta\Delta Ct}$ method, with ribosomal mRNA *18S* as the internal control. The reverse and forward primers of *18S* are given in Table 1.

2.5. In situ hybridization

Whole-mount in situ hybridization was done following the protocol reported in previous studies (Zhao et al., 2012; Zhao et al., 2013). Briefly, 4% paraformaldehyde was used to fix the embryos before and after the removal of the chorion. Using the designed primers (Table 1), a fragment of *OlHavcr2*, which was amplified by RT-PCR as described above, was subcloned into a pGEMT-easy vector (Promega). Sense and antisense digoxigenin (DIG)-labeled RNA probes were synthesized from the linearized pGEM-*Havcr2* with SP6 or T7 transcriptase by using DIG RNA labeling kit (Roche). The hybridization step was performed overnight at 65 °C. Staining was developed with nitro blue tetrazolium/5-bromo-4-chloro-3-indolyl phosphate (NBT/BCIP). Images were obtained under a stereomicroscope equipped with a digital camera.

2.6. Immune stimulation

The chosen immune stimulants, lipopolysaccharide (LPS, Sigma-Aldrich) and polyinosinic polyribocytidylic acid (polyI:C, Sigma-Aldrich), were respectively dissolved in PBS to make the concentration in 5 μg/μL (Zhao et al., 2014). Totally 150 adults fish were sampled, divided into three equal groups and injected intraperitoneally with 10 μL of PBS, LPS, and polyI:C respectively. At the 1st, 2nd, 3rd, 4th, 7th and 10th-day post-injection (dpi), 5 fish were randomly sampled from each group and dissected for RNA extraction from their immune organs (liver, spleen, kidney, and intestine) followed by qRT-PCR.

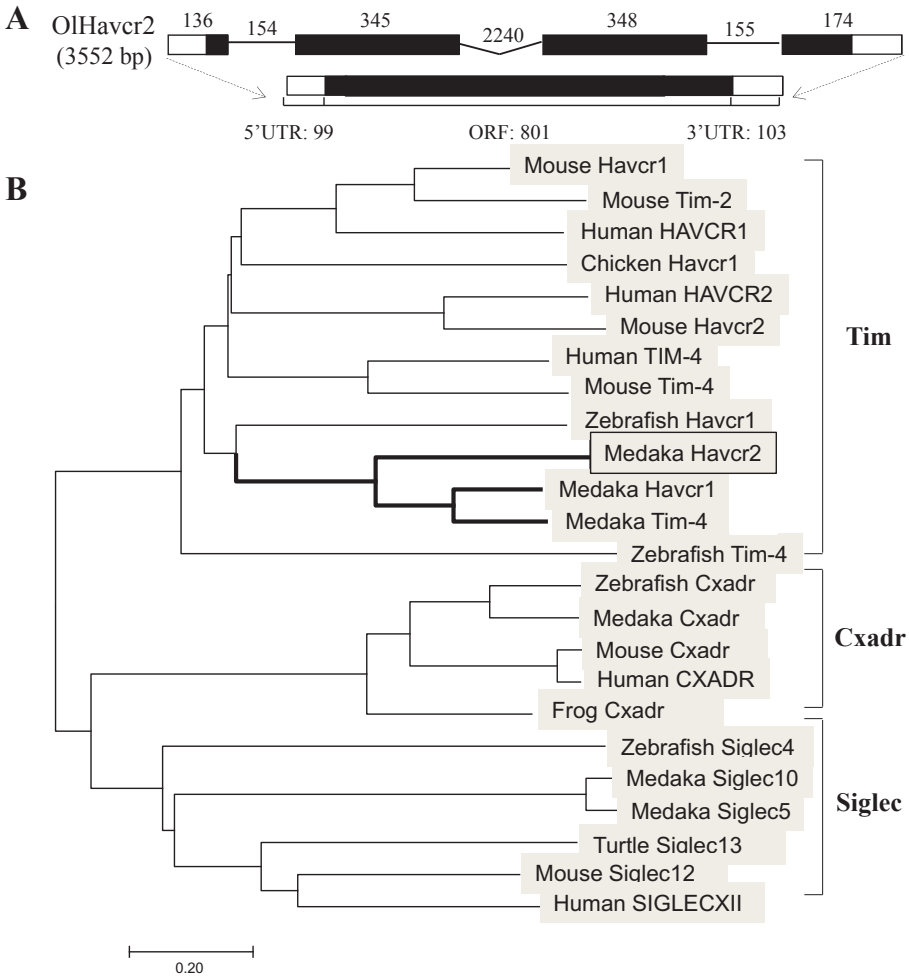

Fig. 1. Phylogenetic tree and *OlHavcr2* genomic structure. (A) *OlHavcr2* exons (mapped as boxes) and introns (mapped as continuous lines) are shown with their respective sizes. ORF and UTR are respectively shown with black and white color. (B) Phylogenetic tree of Tim including Havcr proteins, Cxadr and Siglec proteins. The neighbor-joining method was used to infer the evolutionary history of the proteins (Saitou and Nei, 1987). The optimal tree obtained had the sum of branch length = 6.47528191 as shown in Fig. 1. Drawn to scale, the phylogenetic tree has branch lengths that are uniform with the units of the evolutionary distances used for inference. The p-distance method was used in compiling the evolutionary distances. They are in the units of the number of amino acid differences per site. The analysis involved 24 amino acid sequences. All the positions were eliminated with missing data values and gaps. Evolutionary analyses were conducted in MEGA7.

3. Results

3.1. Phylogenetic analysis

A cDNA of 1003 bp in length was obtained by RT-PCR as described in the method. The cDNA is comprised of a 5′-untranslated region (UTR) of 99 bp, a 3′-UTR of 103 bp and an ORF of 801 bp encoding a protein of 266 amino acids (AA). This gene spans 3, 552 bp located on chromosome 14: 25, 613, 921–25, 618, 182 with 4 exons containing 136 bp, 345 bp, 348 bp and 174 bp respectively, and 3 introns with 154 bp, 2, 240 bp and 155 bp respectively (Fig. 1A). The protein was annotated as Cxadr-like membrane protein (LOC101161824) in the database of GenBank. Blasting this protein in the NCBI database hits three interesting groups of proteins including Tim proteins (containing Havcrs), Cxadrs and sialic acid-binding immunoglobulin-like lectins (Siglecs) (Fig. 1B, Table 2).

The query protein has 76%, 74%, 24%, 29%, and 23% identity to Havcr1 (XP_004076087), Tim-4 (XP_023818151), Cxadr (XP_004076684), Siglec10 (XP_023820428), and Siglec5 (XP_020566001) in medaka. Considering other vertebrates from different taxonomic levels, including zebrafish, turtle, frog, chicken, mouse, and human, the identities of the query protein to Tim proteins range from 49% to 38% (Table 2). The phylogenetic tree established from these proteins reveal that the query protein belongs to the Tim family (Fig. 1B). Hence, the query protein is confirmed as a Tim protein but not a Cxadr protein, nor as a Siglec protein. Similar results are noticeable in medaka where the divergence between the query protein and medaka Havcr1 (0.505) is lower than its divergence from medaka Tim-4 like sequence (0.520) (Supplemental Table 1). This query protein

Table 2
Hits in GenBank and their identity to *OlHavcr2*.

Species	Protein	GenBank ID	Length (aa)	Identity
Oryzias latipes (Medaka)	Cxadr-like	XP_004076716	266	100%
	Havcr1	XP_004076087	248	76%
	Tim-4	XP_023818151	267	74%
	Cxadr	XP_004076684	375	24%
	Siglec10	XP_023820428	662	29%
	Siglec5	XP_020566001	616	23%
Danio rerio (Zebrafish)	Havcr1	NP_001002434	264	46%
	Siglec4	CAF33197	651	42%
	Tim-4	NP_001116089	259	38%
	Cxadr	AAI71370.1	372	23%
Chrysemys picta bellii (Turtle)	Siglec13	XP_023968540	488	27%
Xenopus tropicalis (Frog)	Cxadr	NP_001011084	347	25%
Gallus gallus (Chicken)	Havcr1	NP_001025788	314	44%
Mus musculus (Mouse)	Havcr1	AAL35774	305	49%
	Havcr2	AAI06853	281	42%
	Tim-4	NP_848874	343	39%
	Tim-2	NP_001154827	305	39%
	Siglec12	NP_112458	467	28%
	Cxadr	AAH16457	352	22%
Homo sapiens (Human)	HAVCR2	AFO66593	301	46%
	HAVCR1	BAJ61033	364	40%
	TIM-4	NP_612388	378	38%
	SIGLEC-XII	NP_443729	595	25%
	CXADR	NP_001329	365	21%

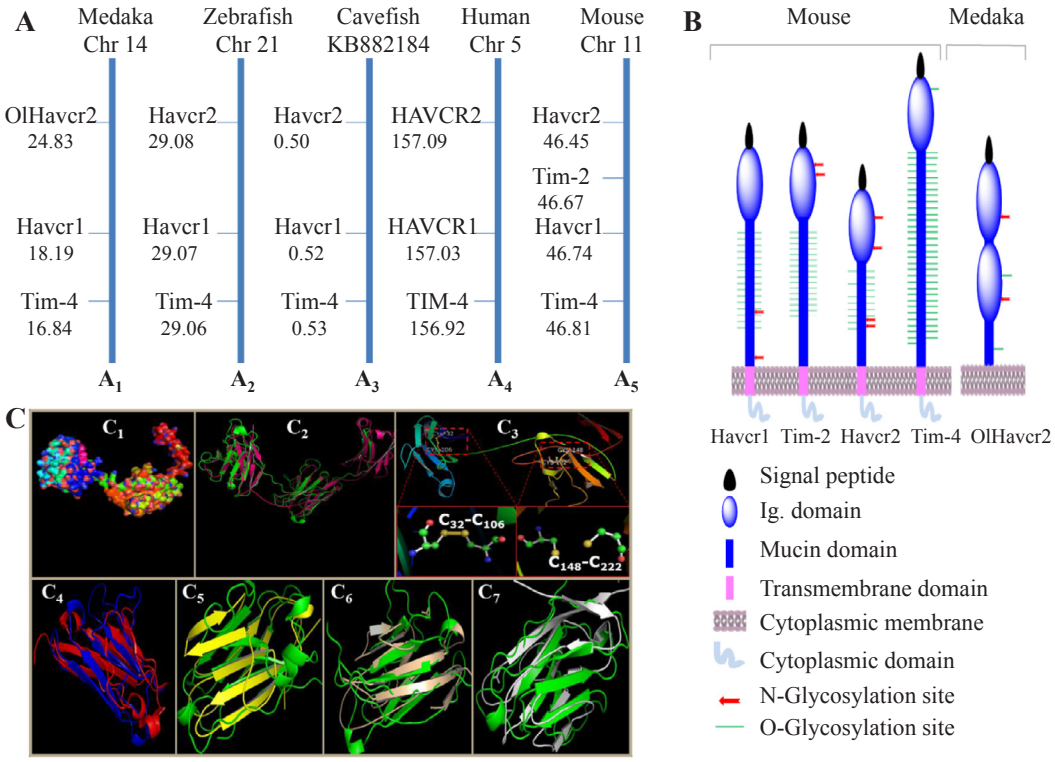

Fig. 2. Characterization of Tim proteins of medaka and other vertebrates. (A) The genes and their positions are shown on the chromosomes of the species schematically. (A_1) medaka chromosome (Chr) 14, (A_2) zebrafish Chr 21, (A_3) cavefish linkage group KB882184, (A_4) human Chr 5, (A_5) mouse Chr 11. (B) Schematic representation of the major structural features of OlHavcr2 and mouse Havcr1, Tim-2, Havcr2, Tim-4 proteins. The signal peptides, Ig-like domains, mucin domains, transmembrane domains and glycosylation sites are approximately illustrated predicted by using the different tools described in materials and methods. (C) Tertiary structure. Structures of the OlHavcr2 (C_1–C_2) and align of OlHavcr2 (one Ig-like domain) to other Tim proteins domains (C_4–C_7) are shown with Pymol. (C_1) The surface structure of OlHavcr2. (C_2) Align OlHavcr2 (green) to the template, 4hjj.1.C (Anti-IL12 Anti-IL18 DFab Light Chain, hot red) by SWISS-MODEL Homology Modelling. (C_3) The conserved cysteine (Cys) residues form the disulfide bridge. (C_4) Align Ig-like domain of OlHavcr2 (blue) to that of mouse Tim-2 (2or7, red). (C_5) Align Ig-like domain of OlHavcr2 (green) to that of Human HAVCR1 (5F70, yellow). (C_6) Align Ig-like domain of OlHavcr2 (green) to 2oyp (Ig-like domain of mouse Havcr2, tint). (C_7) Align Ig-like domain of OlHavcr2 (green) to 3bi9 (Ig-like domain of mouse Tim-4, white).

is identical to mouse Havcr1 and Havcr2 in 49% and 42%, to human HAVCR1 and HAVCR2 in 40% and 46% (Table 2).

To name our query gene correctly, a syntenic assay was performed. In medaka, the query gene containing a predicted gene (ENSORLG00000013602), *Havcr1* (ENSORLG00000000714) and *Tim-4* (ENSORLG00000000711) are mapped on chromosome 14. In zebrafish, cavefish, human and mouse, *Havcr2, Havcr1*, and *Tim-4* are respectively found on chromosome 21, linkage group KB882184, chromosome 5, and chromosome 11 (Fig. 2A). The syntenic assay indicated that the Tim proteins are syntenicly conserved from fish to human. The positions of the Tim proteins are aligned as *Havcr2, Havcr1*, and *Tim-4*, while mouse has an additional *Tim-2* gene between *Havcr2* and *Havcr1* and as an extra duplication of *Havcr1* (Fig. 2A). Thus, our query protein is named as medaka Havcr2 (OlHavcr2).

3.2. Structure of OlHavcr2

OlHavcr2 is a protein of 266 AA containing a signal peptide (17 AA), two immunoglobulin (Ig)-like domains, each of which extends on 110 AA, followed by a very short mucin domain (24 AA) (Fig. 2B). Although this structure is similar to that of Cxadr which possesses two Ig-like domains (Coyne and Bergelson, 2005; Loustalot et al., 2015), sequence analyses reveal it as a Tim protein as described above.

Up to now, the known Tim proteins share the common structural characteristics that consist of an N-terminal Ig-like domain, a transmembrane domain, a mucin domain that varies in length, O-glycosylation sites, N-glycosylation sites and a cytoplasmic tail (Freeman et al., 2010; McIntire et al., 2004). OlHavcr2 possesses the O-glycosylation sites (O-$Glyc_{188}$, O-$Glyc_{255}$) and N-glycosylation sites (N-$Glyc_{95}$ and N-$Glyc_{211}$). The mucin domain of OlHavcr2 is short (24 AA), compared with those of mouse Tim-1 to Tim-4 whose sizes are 108, 103, 61 and 146 AA respectively (Fig. 2B). Different from mammal Tim proteins, OlHavcr2 has two Ig-like domains and lacks a cytoplasmic tail and transmembrane domain, indicating that it is a protein secreted out from the cytoplasm and located on the cell surface. These results suggest that OlHavcr2 is involved in intercellular signaling or recognition (Fig. 2B). These unique characters deserve further studies to clarify the function and the mechanism of OlHavcr2 in cell signaling.

OlHavcr2 tertiary structure was modeled using SWISS-MODEL Homology Modelling with anti-IL12 anti-IL18 DFab light chain (4hjj.1.C) as the template. The overview of OlHavcr2 tertiary structure reveals that this protein is constituted of two Ig-like domains. The structures were selected for further analysis and comparison to mouse Havcr1, Tim-2, Havcr2 and Tim-4 (Fig. 2C_1, C_2). OlHavcr2 contains a total of eight cysteine residues including six conserved cysteine residues found in Tim proteins (Xu et al., 2016). In OlHavcr2, four cysteine residues (Cys_{32}, Cys_{45}, Cys_{56} and Cys_{106}) are in the 1st Ig-like domain, and other four cysteine residues (Cys_{148}, Cys_{161}, Cys_{172} and Cys_{222}) are in the 2nd Ig-like domain. The disulfide bridge exists in the 1st Ig-like domain (Cys_{32}-Cys_{106}), while there is no disulfide bridge in the 2nd Ig-like domain (Fig. 2C_3). Furthermore, one of the two Ig-like domains of OlHavcr2 was chosen arbitrarily to be superimposed on the Ig-like domains of human HAVCR1, mouse Tim-2, Havcr2 and Tim-4. In both 3D structures, alignment reveals that the anti-parallel β-strands in

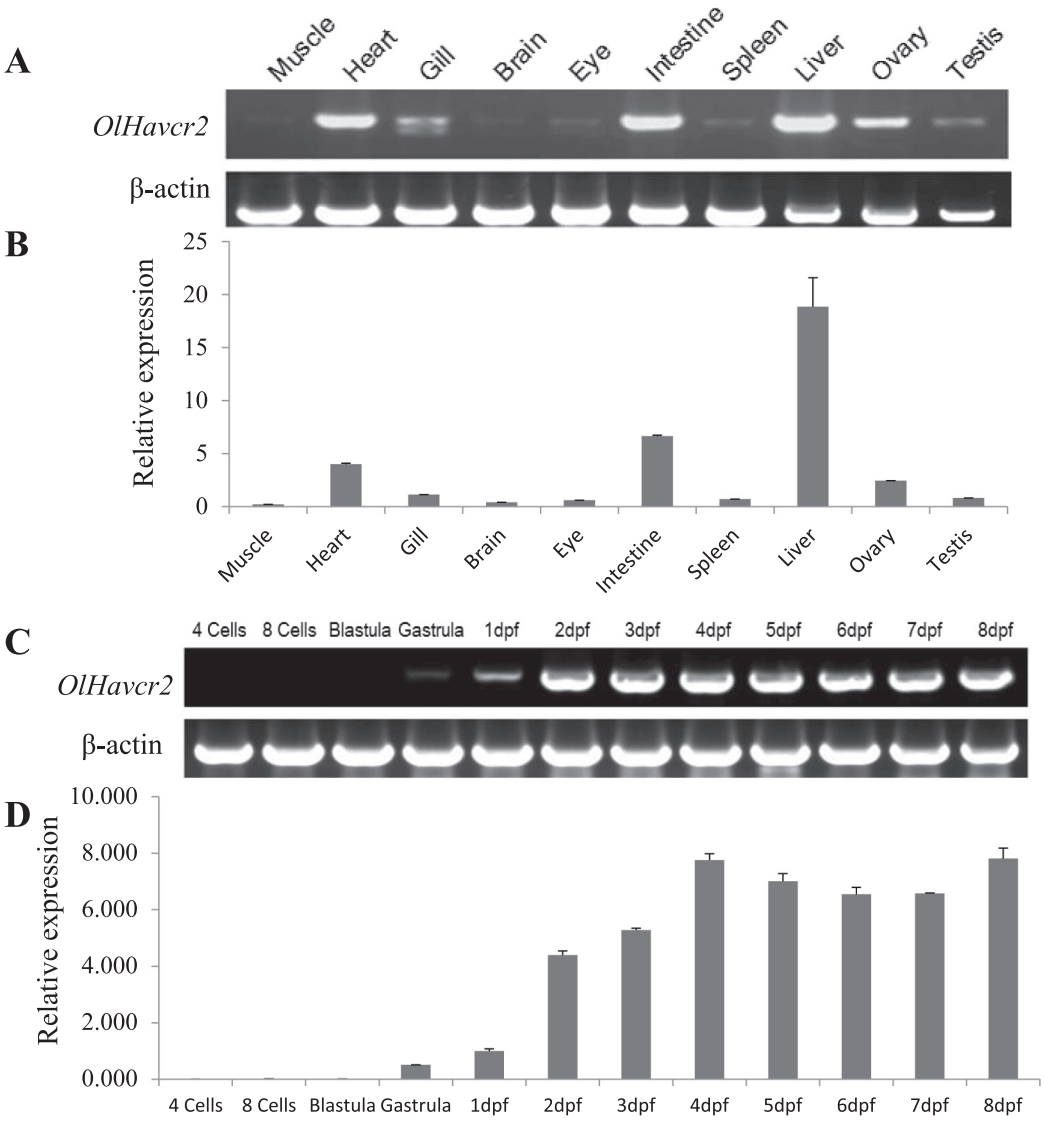

Fig. 3. Relative expression of *OlHavcr2*. (A) The expression of *OlHavcr2* mRNA in different tissues of medaka measured by RT-PCR, with *β-actin* as the internal control. (B) QRT-PCR results of *OlHavcr2* expression in adult tissues of medaka. The relative expression levels were normalized with *18S* levels. n = 3. (C) Expression of *OlHavcr2* during embryonic development by RT-PCR, with *β-actin* as the internal control. (D) Relative mRNA levels of *OlHavcr2* during embryogenesis measured by qRT-PCR and normalized with *18S* levels. n = 3. dpf, day (s) post fertilization.

stacked pleated β-sheets and the α-helix structures are structurally homologous. The corresponding amino acids of the OlHavcr2 Ig-like domain to those of human HAVCR1, mouse Tim-2, Havcr2 and Tim-4 are close to one another (Fig. 2C_4–C_7).

3.3. Expression of OlHavcr2 in adult tissues of medaka

RT-PCR results exhibited that *OlHavcr2* mRNA was manifested in all checked tissues including muscle, heart, gill, brain, eye, intestine, spleen, liver, testis and ovary (Fig. 3A). In fact, *OlHavcr2* exhibited its strong expression in the liver. Moderate mRNA expression of *OlHavcr2* was identified in the intestine, heart, and ovary, whereas weak signals of *OlHavcr2* were identified in the muscle, gill, brain, eye, spleen, and testis. The control (*β-actin*) was clear and almost the same in all checked tissues, suggesting that the results were not an error in the RT-PCR reaction (Fig. 3A). QRT-PCR confirmed the tissue distribution pattern of *OlHavcr2* in adult (Fig. 3B). These findings suggest a ubiquitous expression of *OlHavcr2* in adult tissues.

3.4. Expression of OlHavcr2 during embryonic development

RT-PCR results revealed that there were no remarkable signals of *OlHavcr2* from 8-cells to blastula stage of medaka embryos. *OlHavcr2* was weakly detected from gastrula stage and was moderate on 1st day post-fertilization (dpf). Interestingly, a strong band was noteworthy from 2 dpf to 8 dpf (Fig. 3C). QRT-PCR confirmed these results. No significant expression of *OlHavcr2* could be detected from 4-cells to blastula stage. It is evident that the expression begins from gastrula stage, reaches peak in 4 dpf, and is consistent until hatching (Fig. 3D).

To further explore the spatial-temporal expression of *OlHavcr2* during embryonic development, in situ hybridization was performed. At 1 dpf stage, *OlHavcr2* was detected in the embryonic body. The signals of *OlHavcr2* were observed in the forebrain, midbrain, hindbrain, and eye (Fig. 4a and b). Surprisingly, the signals of *OlHavcr2* were mainly identified in the yolk sac from 1 dpf to the fry (Fig. 4). These results suggest that *OlHavcr2* is highly expressed in the blood system given that the yolk sac is important in early embryonic blood supply (Palmentieri et al., 2006). In the fry, *OlHavcr2* expression was detected in the blood system and the heart (Fig. 4d).

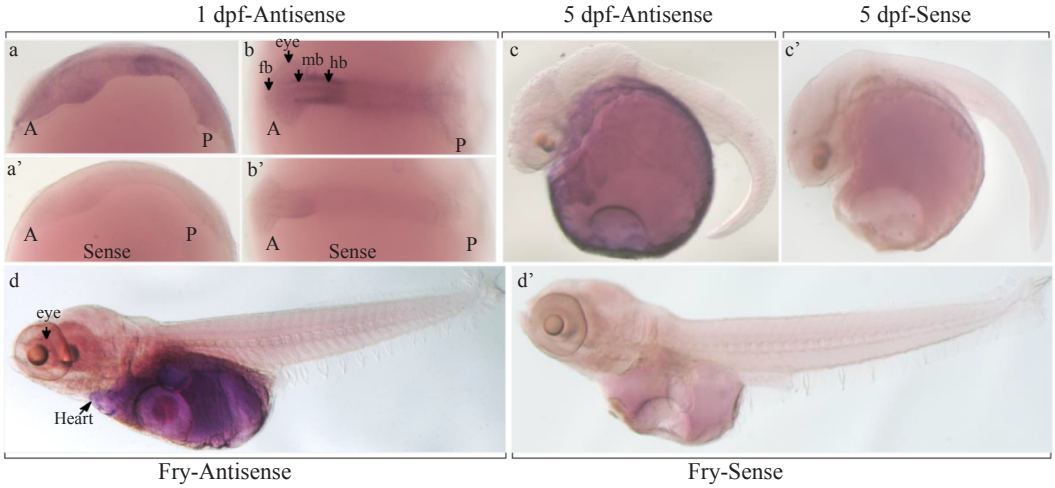

Fig. 4. Expressions of *OlHavcr2* during embryonic development of medaka detected using in situ hybridization. a–d, images denote antisense probe results. a′-d′, the sense probe was used as the control and showed no signal. a-a′, lateral view; b-b′, dorsal view at 1 dpf (stage 19). c–c′, 5 dpf stage. d-d′, fry with lateral view. A, anterior; fb, fore brain; hb, hind brain; mb, mid brain; P, posterior.

3.5. Immune response of OlHavcr2 in immune organs of medaka

After intraperitoneal injection of immune stimulants, LPS and polyI:C, in adult fish, *OlHavcr2* expression in different immune organs including the liver, spleen, kidney, and intestine was detected from one day to another (Fig. 5).

In the liver, *OlHavcr2* was significantly increased at 1 and 2 dpi ($p < 0.05$), reached a peak at 3 dpi ($p < 0.001$) and then decreased under the control level from 7 dpi of LPS. After polyI:C stimulation, *OlHavcr2* was significantly increased at 1 dpi ($p < 0.001$), reached a peak at 2 dpi ($p < 0.001$) and decreased to the control level from 3 dpi (Fig. 5A).

In the intestine, *OlHavcr2* expression was significantly increased at 2 and 3 dpi ($p < 0.01$) and exhibited the highest level at 4 dpi ($p < 0.001$) by LPS. After polyI:C stimulation, the expression of *OlHavcr2* in the intestine reached the peak significantly at 1 dpi ($p < 0.001$) and kept at high level until 3 dpi ($p < 0.01$). However, *OlHavcr2* expression in polyI:C group was less than the control level at

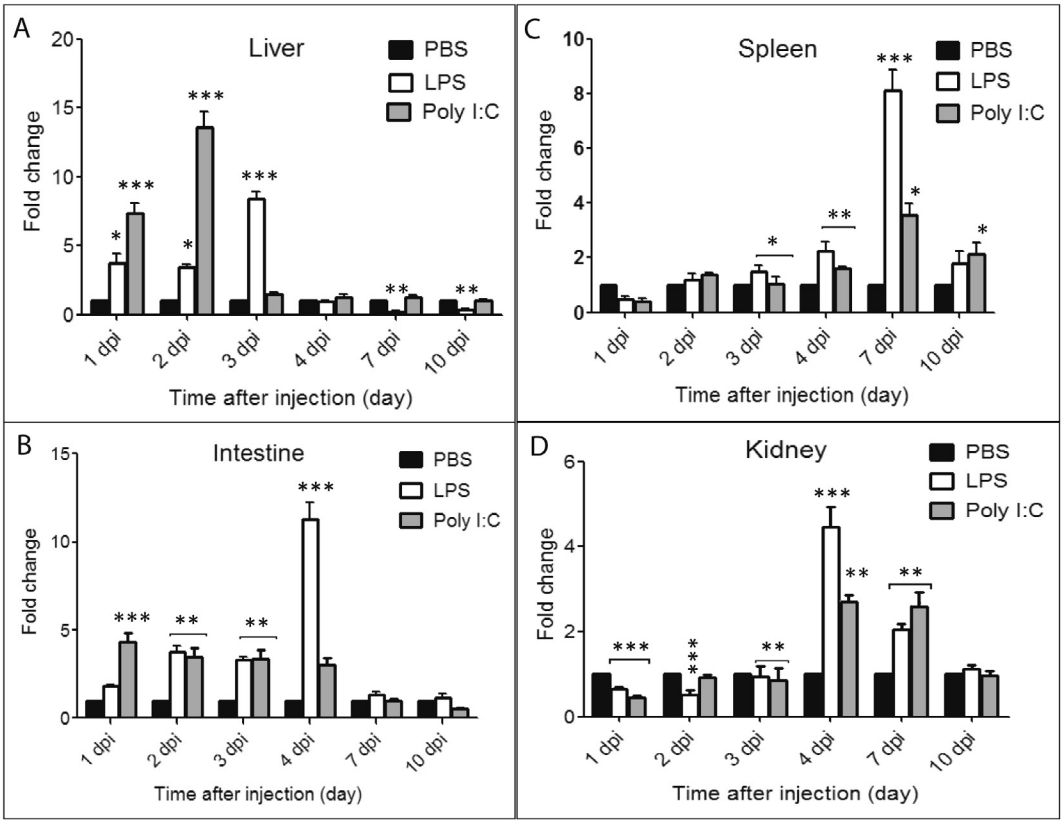

Fig. 5. Expression of *OlHavcr2* after immune stimulation. The data were analyzed in one-way ANOVA with homogeneity of variance test using SPSS V.20.0 software. n = 3. *, $P < 0.05$; **, $P < 0.01$; ***, $P < 0.001$.

10 dpi (Fig. 5B).

After LPS stimulation, the spleen exhibited significant increase of *OlHavcr2* at 3 dpi ($p < 0.05$), 4 dpi ($p < 0.01$) and showed the highest level at 7 dpi ($p < 0.001$). After polyI:C stimulation, the expression of *OlHavcr2* in the spleen decreased at 1 dpi, but significantly increased at 3 dpi ($p < 0.05$) and 4 dpi ($p < 0.01$) to reach the highest level at 7 dpi ($p < 0.05$), and slightly dropped at 10 dpi ($p < 0.05$) (Fig. 5C).

In the kidney, the LPS stimulation exhibited decrease of *OlHavcr2* expression at 1 to 3 dpi, but the significant increase of *OlHavcr2* was detected at 4 dpi ($p < 0.001$) and slightly decreased at 7 dpi ($p < 0.01$). Like LPS, polyI:C stimulation exhibited decrease of *OlHavcr2* expression at 1 to 3 dpi, the significantly high expression of *OlHavcr2* revealed at 4 dpi ($p < 0.01$) and 7 dpi ($p < 0.01$) (Fig. 5D).

4. Discussion

In the present study, *OlHavcr2* was identified. *Ol*Havcr2 has the fundamental characteristics such as a signal peptide, 2 Ig-like domains, 2 O-glycosylation sites, 2 N-glycosylation sites, and a mucin domain but without the transmembrane and cytoplast domains. *OlHavcr2* mRNA is ubiquitously expressed in adult fish. During embryonic development, *OlHavcr2* mRNA begins to manifest from gastrula stage indicating that *OlHavcr2* is a zygotic gene. In addition, *OlHavcr2* expression in the immune organs responds to the stimulation of LPS and polyI:C in medaka.

OlHavcr2 differs from the other Tim proteins particularly with two Ig-like domains and lacks cytoplasmic and transmembrane domains. OlHavcr2 is a protein on the cell surface and resembles to the soluble form of Havcr2 described previously in mice (Monney et al., 2002). It is still unclear whether OlHavcr2 has the same function as that of mouse Havcr2.

OlHavcr2 is expressed ubiquitously in adult tissues like zebrafish *Havcr2* which was detected in multiple tissues (Yin et al., 2016). *OlHavcr2* is detected in the immune organs and is predominantly expressed in the yolk sac during embryogenesis suggesting that it may be implicated in the mechanism of the blood system and in immunity. The experiments with immune stimulants, LPS and polyI:C give further evidences that *OlHavcr2* is possibly involved in the innate and adaptive immunity of fish. The early increase of *OlHavcr2* responding to LPS or poly I:C could be detected in 1 or 2 days in the liver and intestine. The late increase of *OlHavcr2* expression could be detected in 7 days in the spleen and kidney. The early response may reveal the function of OlHavcr2 in the innate immunity, and the late increase of *OlHavcr2* suggests the role of OlHavcr2 in the adaptive immunity.

OlHavcr2 may function in the innate and adaptive immune in fish as its homologs in mice and human. In human and mice, Havcr2 exists in CD4+ interferon gamma and CD8+ lymphocytes (Hastings et al., 2009; Koohini et al., 2018; Lu et al., 2017; Sabatos et al., 2003) and takes part in immune regulation (Banerjee and Kane, 2018; DeKruyff et al., 2010; Hou et al., 2017; Nakayama et al., 2018; Wu et al., 2017; Zhang et al., 2011). Havcr2 play a crucial role in innate and adaptive immune response has been reported numerously in mice and human (Gorman and Colgan, 2014). A specific study would be necessary to clarify the mechanism by which OlHavcr2 intervenes in innate and adaptive immune system.

In summary, *OlHavcr2* is identified in medaka with the unique structures, and is ubiquitously expressed in adult, and is a zygotic gene mainly expressed in the blood system of the embryos. OlHavcr2 structure exhibits resemblances and differences comparing to other members of Tim proteins. Its unique characteristics constitute a subject of future research to clarify the specific role of OlHavcr2 in medaka.

Acknowledgment

This work was supported by National Natural Science Foundation of China, Grant Nos. 31672284, 31272645 to HZ.

Appendix A. Supplementary data

Supplementary data to this article can be found online at https://doi.org/10.1016/j.ygcen.2018.10.023.

References

Anderson, A.C., Anderson, D.E., Bregoli, L., Hastings, W.D., Kassam, N., Lei, C., Chandwaskar, R., Karman, J., Su, E.W., Hirashima, M., Bruce, J.N., Kane, L.P., Kuchroo, V.K., Hafler, D.A., 2007. Promotion of tissue inflammation by the immune receptor tim-3 expressed on innate immune cells. Science (80-) 318, 1141–1143. https://doi.org/10.1126/science.1148536.

Banerjee, H., Kane, L.P., 2018. Immune regulation by Tim-3. F1000Research 7 (316). https://doi.org/10.12688/f1000research.13446.1.

Blom, N., Sicheritz-Pontén, T., Gupta, R., Gammeltoft, S., Brunak, S., 2004. Prediction of post-translational glycosylation and phosphorylation of proteins from the amino acid sequence. Proteomics. https://doi.org/10.1002/pmic.200300771.

Boenisch, O., D'Addio, F., Watanabe, T., Elyaman, W., Magee, C.N., Yeung, M.Y., Padera, R.F., Rodig, S.J., Murayama, T., Tanaka, K., Yuan, X., Ueno, T., Jurisch, A., Mfarrej, B., Akiba, H., Yagita, H., Najafian, N., 2010. TIM-3: a novel regulatory molecule of alloimmune activation. J. Immunol. 185, 5806–5819. https://doi.org/10.4049/jimmunol.0903435.

Chae, S.C., Park, Y.R., Shim, S.C., Yoon, K.S., Chung, H.T., 2004. The polymorphisms of Th1 cell surface gene Tim-3 are associated in a Korean population with rheumatoid arthritis. Immunol. Lett. 95, 91–95. https://doi.org/10.1016/j.imlet.2004.06.008.

Coyne, C.B., Bergelson, J.M., 2005. CAR: a virus receptor within the tight junction. Adv. Drug Deliv. Rev. 57, 869–882. https://doi.org/10.1016/j.addr.2005.01.007.

DeKruyff, R.H., Bu, X., Ballesteros, A., Santiago, C., Chim, Y.-L.E., Lee, H.-H., Karisola, P., Pichavant, M., Kaplan, G.G., Umetsu, D.T., Freeman, G.J., Casasnovas, J.M., 2010. T cell/transmembrane, Ig, and mucin-3 allelic variants differentially recognize phosphatidylserine and mediate phagocytosis of apoptotic cells. J. Immunol. 184, 1918–1930. https://doi.org/10.4049/jimmunol.0903059.

Feng, Z.M., Guo, S.M., 2016. Tim-3 facilitates osteosarcoma proliferation and metastasis through the NF-κB pathway and epithelial-mesenchymal transition. Genet. Mol. Res. 15, 1–9. https://doi.org/10.4238/gmr.15037844.

Fourcade, J., Sun, Z., Benallaoua, M., Guillaume, P., Luescher, I.F., Sander, C., Kirkwood, J.M., Kuchroo, V., Zarour, H.M., 2010. Upregulation of Tim-3 and PD-1 expression is associated with tumor antigen–specific $CD8^+$ T cell dysfunction in melanoma patients. J. Exp. Med. 207, 2175–2186. https://doi.org/10.1084/jem.20100637.

Freeman, G.J., Casasnovas, J.M., Umetsu, D.T., Dekruyff, R.H., 2010. TIM genes: a family of cell surface phosphatidylserine receptors that regulate innate and adaptive immunity. Rev. Immunol. https://doi.org/10.1111/j.0105-2896.2010.00903.x.

Gao, X., Zhu, Y., Li, G., Huang, H., Zhang, G., Wang, F., Sun, J., Yang, Q., Zhang, X., Lu, B., 2012. TIM-3 expression characterizes regulatory T cells in tumor tissues and is associated with lung cancer progression. PLoS One 7, 1–8. https://doi.org/10.1371/journal.pone.0030676.

Gorman, J.V., Colgan, J.D., 2014. Regulation of T cell responses by the receptor molecule Tim-3. Res Immunol. https://doi.org/10.1007/s12026-014-8524-1.

Hastings, W.D., Anderson, D.E., Kassam, N., Koguchi, K., Greenfield, E.A., Kent, S.C., Zheng, X.X., Strom, T.B., Hafler, D.A., Kuchroo, V.K., 2009. TIM-3 is expressed on activated human CD4+ T cells and regulates Th1 and Th17 cytokines. Eur. J. Immunol. 39, 2492–2501. https://doi.org/10.1002/eji.200939274.

Hou, N., Jiang, N., Zou, Y., Piao, X., Liu, S., Li, S., Chen, Q., 2017. Down-regulation of Tim-3 in monocytes and macrophages in Plasmodium infection and its association with parasite clearance. Front. Microbiol. 8, 1–10. https://doi.org/10.3389/fmicb.2017.01431.

Hu, X.-H., Tang, M.-X., Mor, G., Liao, A.-H., 2016. Tim-3: Expression on immune cells and roles at the maternal-fetal interface. J. Reprod. Immunol. 118, 92–99. https://doi.org/10.1016/j.jri.2016.10.113.

Takashi, Iwamatsu, 1994. Stages of normal development in the medaka Oryzias latipes. Zoolog. Sci. 11, 825–839.

Japp, A.S., Kursunel, M.A., Meier, S., Mälzer, J.N., Li, X., Rahman, N.A., Jekabsons, W., Krause, H., Magheli, A., Klopf, C., Thiel, A., Frentsch, M., 2015. Dysfunction of PSA-specific CD8+T cells in prostate cancer patients correlates with CD38 and Tim-3 expression. Cancer Immunol. Immunother. 64, 1487–1494. https://doi.org/10.1007/s00262-015-1752-y.

Koohini, Z., Hossein-Nataj, H., Mobini, M., Hosseinian-Amiri, A., Rafiei, A., Asgarian-Omran, H., 2018. Analysis of PD-1 and Tim-3 expression on CD4+ T cells of patients with rheumatoid arthritis; negative association with DAS28. Clin. Rheumatol. 1, 1–9. https://doi.org/10.1007/s10067-018-4076-4.

Kumar, S., Stecher, G., Tamura, K., 2016. MEGA7: molecular evolutionary genetics analysis version 7.0 for bigger datasets. Mol. Biol. Evol. 33, 1870–1874. https://doi.org/10.1093/molbev/msw054.

Letunic, I., Doerks, T., Bork, P., 2015. SMART: recent updates, new developments and status in 2015. Nucleic Acids Res. 43, D257–D260. https://doi.org/10.1093/nar/gku949.

Li, Z., Ju, Z., Frieri, M., 2013. The T-cell immunoglobulin and mucin domain (Tim) gene family in asthma, allergy, and autoimmunity. Allergy Asthma Proc. 34. https://doi.org/10.2500/aap.2013.34.3646.

Li, Z., Liu, X., Guo, R., Wang, P., 2017. TIM-3 plays a more important role than PD-1 in the functional impairments of cytotoxic T cells of malignant Schwannomas. Tumour Biol. 39https://doi.org/10.1177/1010428317698352. 1010428317698352.

Liu, Y., Wang, J., Wang, L., Wang, B., Yang, S., Wang, Q., Luo, J., Feng, X., Yang, X., Lu, Y., Roggendorf, M., Lu, M., Yang, D., Liu, J., 2017. Molecular cloning,

characterization and expression analysis of Tim-3 and Galectin-9 in the woodchuck model. Mol. Immunol. 83, 127–136. https://doi.org/10.1016/j.molimm.2017.01.018.

Loustalot, F., Kremer, E.J., Salinas, S., 2015. The intracellular domain of the coxsackievirus and adenovirus receptor differentially influences adenovirus entry. J. Virol. 89, 9417–9426. https://doi.org/10.1128/JVI.01488-15.

Lu, X., Yang, L., Yao, D., Wu, X., Li, J., Liu, X., Deng, L., Huang, C., Wang, Y., Li, D., Liu, J., 2017. Tumor antigen-specific CD8 + T cells are negatively regulated by PD-1 and Tim-3 in human gastric cancer. Cell. Immunol. 313, 43–51. https://doi.org/10.1016/j.cellimm.2017.01.001.

McIntire, J.J., Umetsu, D.T., DeKruyff, R.H., 2004. TIM-1, a novel allergy and asthma susceptibility gene. Springer Semin. Immunopathol. 25, 335–348. https://doi.org/10.1007/s00281-003-0141-3.

Monney, L., Sabatos, C.A., Gaglia, J.L., Ryu, A., Waldner, H., Chernova, T., Manning, S., Greenfield, E.A., Coyle, A.J., Sobel, R.A., Freeman, G.J., Kuchroo, V.K., 2002. Th1-specific cell surface protein Tim-3 regulates macrophage activation and severity of an autoimmune disease. Nature 415, 536–541. https://doi.org/10.1038/415536a.

Nakae, S., Iikura, M., Suto, H., Akiba, H., Umetsu, D.T., Rosemarie, H., Saito, H., Galli, S.J., Dc, W., Dekruyff, R.H., 2007a. TIM-1 and TIM-3 enhancement of Th2 cytokine production by mast cells Brief report TIM-1 and TIM-3 enhancement of Th2 cytokine production by mast cells. Blood 110, 2565–2568. https://doi.org/10.1182/blood-2006-11-058800.

Nakae, S., Iwakura, Y., Suto, H., Galli, S.J., 2007b. Phenotypic differences between Th1 and Th17 cells and negative regulation of Th1 cell differentiation by IL-17. J. Leukoc. Biol. 81, 1258–1268. https://doi.org/10.1189/jlb.1006610.

Nakayama, M., Akiba, H., Takeda, K., Kojima, Y., Hashiguchi, M., Azuma, M., Yagita, H., Okumura, K., 2018. Tim-3 mediates phagocytosis of apoptotic cells and cross-presentation. Blood 113, 3821–3831. https://doi.org/10.1182/blood-2008-10-185884. The.

Nielsen, H., Engelbrecht, J., Brunak, S., Von Heijne, G., 1997. Identification of prokaryotic and enkaryotic signal peptides and prediction of their cleavage sites. Protein Eng. 10, 1–6.

Palmentieri, B., de Sio, I., La Mura, V., Masarone, M., Vecchione, R., Bruno, S., Torella, R., Persico, M., 2006. The role of bright liver echo pattern on ultrasound B-mode examination in the diagnosis of liver steatosis. Dig. Liver Dis. 38, 485–489. https://doi.org/10.1016/j.dld.2006.03.021.

Rodriguez-Manzanet, R., Dekruyff, R., Kuchroo, V.K., Umetsu, D.T., 2009. The costimulatory role of TIM molecules. Rev. Immunol. https://doi.org/10.1111/j.1600-065X.2009.00772.x.

Sabatos, C.A., Chakravarti, S., Cha, E., Schubart, A., Sánchez-Fueyo, A., Zheng, X.X., Coyle, A.J., Strom, T.B., Freeman, G.J., Kuchroo, V.K., 2003. Interaction of Tim-3 and Tim-3 ligand regulates T helper type 1 responses and induction of peripheral tolerance. Nat. Immunol. 4, 1102–1110. https://doi.org/10.1038/ni988.

Saitou, N., Nei, M., 1987. The neighbor-joining method – a new method for reconstructing phylogenetic trees. Mol. Biol. Evol. 4, 406–425.

Sánchez-Fueyo, A., Tian, J., Picarella, D., Domenig, C., Zheng, X.X., Sabatos, C.A., Manlongat, N., Bender, O., Kamradt, T., Kuchroo, V.K., Gutiérrez-Ramos, J.C., Coyle, A.J., Strom, T.B., 2003. Tim-3 inhibits T helper type 1-mediated auto- and alloimmune responses and promotes immunological tolerance. Nat. Immunol. 4, 1093–1101. https://doi.org/10.1038/ni987.

Schultz, J., Milpetz, F., Bork, P., Ponting, C.P., 1998. SMART, a simple modular architecture research tool: Identification of signaling domains. Proc. Natl. Acad. Sci. 95, 5857–5864. https://doi.org/10.1073/pnas.95.11.5857.

Shayan, G., Srivastava, R., Li, J., Schmitt, N., Kane, L.P., Ferris, R.L., 2017. Adaptive resistance to anti-PD1 therapy by tim-3 upregulation is mediated by the PI3k-akt pathway in head and neck cancer. Oncoimmunology 6, 1–11. https://doi.org/10.1080/2162402X.2016.1261779.

Steentoft, C., Vakhrushev, S.Y., Joshi, H.J., Kong, Y., Vester-Christensen, M.B., Schjoldager, K.T.B.G., Lavrsen, K., Dabelsteen, S., Pedersen, N.B., Marcos-Silva, L., Gupta, R., Paul Bennett, E., Mandel, U., Brunak, S., Wandall, H.H., Levery, S.B., Clausen, H., 2013. Precision mapping of the human O-GalNAc glycoproteome through SimpleCell technology. EMBO J. 32, 1478–1488. https://doi.org/10.1038/emboj.2013.79.

Veenstra, R.G., Taylor, P.A., Zhou, Q., Panoskaltsis-mortari, A., Hirashima, M., Flynn, R., Liu, D., Anderson, A.C., Strom, T.B., Kuchroo, V.K., Bruce, R., Blazar, B.R., 2012. Contrasting acute graft-versus-host disease effects of Tim-3/galectin-9 pathway blockade dependent upon the presence of donor regulatory T cells. Survival (Lond.) 120, 682–690. https://doi.org/10.1182/blood-2011-10-387977.

Wang, Z., Sun, D., Chen, G., Li, G., Dou, S., Wang, R., Xiao, H., Hou, C., Li, Y., Feng, J., Shen, B., Han, G., 2017. Tim-3 inhibits macrophage control of Listeria monocytogenes by inhibiting Nrf2. Sci. Rep. 7. https://doi.org/10.1038/srep42095.

Wu, R., Long, L., Chen, Q., Wu, X., Zhu, J., Zhou, B., Cheng, J., 2017. Effects of tim-3 silencing on the viability of fibroblast-like synoviocytes and lipopolysaccharide-induced inflammatory reactions. Exp. Ther. Med. 14, 2721–2727. https://doi.org/10.3892/etm.2017.4819.

Xu, X., Hu, J., Ma, J., Nie, L., Shao, T., Xiang, L., Shao, J., 2016. Essential roles of TIM-1 and TIM-4 homologs in adaptive humoral immunity in a zebrafish model. J. Immunol. 196, 1686–1699. https://doi.org/10.4049/jimmunol.1501736.

Yan, J., Zhang, Y., Zhang, J.-P., Liang, J., Li, L., Zheng, L., 2013. Tim-3 expression defines regulatory T cells in human tumors. PLoS One 8, e58006. https://doi.org/10.1371/journal.pone.0058006.

Yang, X., Jiang, X., Chen, G., Xiao, Y., Geng, S., Kang, C., Zhou, T., Li, Y., Guo, X., Xiao, H., Hou, C., Wang, R., Lin, Z., Li, X., Feng, J., Ma, Y., Shen, B., Li, Y., Han, G., 2013. T cell Ig Mucin-3 promotes homeostasis of sepsis by negatively regulating the TLR response. J. Immunol. 190, 2068–2079. https://doi.org/10.4049/jimmunol.1202661.

Yang, Z.Z., Grote, D.M., Ziesmer, S.C., Niki, T., Hirashima, M., Novak, A.J., Witzig, T.E., Ansell, S.M., 2012. IL-12 upregulates TIM-3 expression and induces T cell exhaustion in patients with follicular B cell non-Hodgkin lymphoma. J. Clin. Invest. 122, 1271–1282. https://doi.org/10.1172/JCI59806.

Yin, W., Naini, S.M., Chen, G., Hentschel, D.M., Humphreys, B.D., Bonventre, J.V., 2016. Mammalian target of rapamycin mediates kidney injury molecule 1-dependent tubule injury in a surrogate model. J. Am. Soc. Nephrol. 1943–1957. https://doi.org/10.1681/ASN.2015050500.

Zhang, H., Xiang, R., Wu, B., Li, J., Luo, G., 2017. T-cell immunoglobulin mucin-3 expression in invasive ductal breast carcinoma: clinicopathological correlations and association with tumor infiltration by cytotoxic lymphocytes. Mol. Clin. Oncol. 7, 557–563. https://doi.org/10.3892/mco.2017.1360.

Zhang, Y., Ma, C.J., Wang, J.M., Ji, X.J., Wu, X.Y., Jia, Z.S., Moorman, J.P., Yao, Z.Q., 2011. Tim-3 negatively regulates IL-12 expression by monocytes in HCV infection. PLoS One 6. https://doi.org/10.1371/journal.pone.0019664.

Zhao, H., Cui, J., Wang, Y., Liu, X., Zhao, D., Duan, J., 2012. Spatial-temporal expression of pum1 and pum2 in medaka Oryzias latipes. J. Fish Biol. 80, 100–109. https://doi.org/10.1111/j.1095-8649.2011.03153.x.

Zhao, H., Guan, G., Duan, J., Cheng, N., Wang, J., Matsuda, M., Paul-Prasanth, B., Nagahama, Y., 2013. Ol4E-T, a eukaryotic translation initiation factor 4E-binding protein of medaka fish (Oryzias latipes), can interact with Nanos3 and vasa in vitro. J. Exp. Zool. Part B Mol. Dev. Evol. 320, 10–21. https://doi.org/10.1002/jez.b.22465.

Zhao, H., Zhang, X., Cheng, N., Duan, J., Wang, J., Nagahama, Y., Zhong, X., Zhou, Q., Wang, Y., 2014. Identification and expression profiles of prdm1 in medaka Oryzias latipes. Mol. Biol. Rep. 41, 617–626. https://doi.org/10.1007/s11033-013-2899-2.